ManifoldEM (Beta) Python User Manual

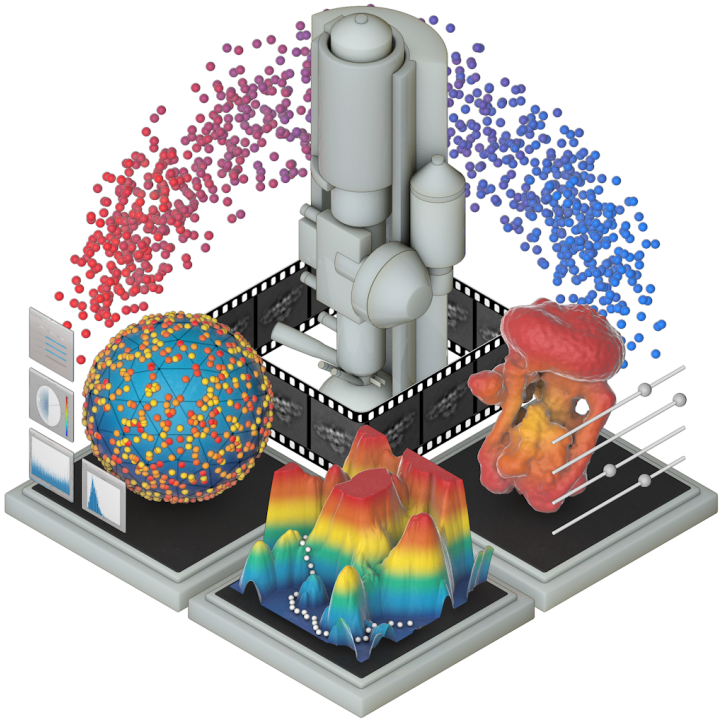

Evan Seitz, Ghoncheh Mashayekhi, Hstau Liao, Suvrajit Maji,

Peter Schwander*, Abbas Ourmazd* and Joachim Frank*

Version 0.2.0-beta

October 19, 2021

Contents

1 Introduction

This tutorial provides an overview of ManifoldEM (Beta version) in Python 3 for determination of cryo-EM conformational continua, as was first introduced by Dashti et al. (2014). The tutorial covers the entire manifold analysis workflow, from data preparation to construction of free-energy landscape. Carefully going through this tutorial will prepare you for running ManifoldEM on your own data. This tutorial uses a demo[†] data set provided by Mashayekhi (2020), which is a small subset of the experimental data provided by Amédée des Georges et al. (2016) used in the functional pathway analysis of ryanodine receptor 1 (RyR1; Dashti et al., 2020). As such, this data set should only be used for help in understanding the software and for training purposes. If you have any questions about ManifoldEM after reading this entire document, carefully check the ManifoldEM Python GitHub forum for similar inquiries or – if no similar posts exist – create a new thread detailing your inquiry. As well, if you find any errors while reading this document, please let us know.

As an introductory overview, we have provided a video demonstration of the ManifoldEM Python GUI, which was presented at the 2019 Computational Cryo-EM workshop (Flatiron Institute). The data set shown for this demonstration is V-ATPase, which was provided by Zhao et al. (2015): https://www.dropbox.com/s/pe106oizw4p7uyb/GUI_Overview_VATPase.mp4?dl=0

[†] If the above link to the demo data set provides any difficulty, please try this mirror.

1.1 ManifoldEM Motivation

Molecular machines are macromolecular assemblies – consisting of proteins or nucleoproteins – that perform basic life functions and undergo numerous conformational changes in the course of their work cycles. For some molecular machines, such as the ribosome, it has been possible to develop *in vitro* systems with all components necessary to run productive work cycles delivering the product, in this instance a protein. Even though the atomistic composition of molecules ultimately defines a finite step size, the states form a virtual continuum due to the complexity of the structures involved and the large number of steps in their interactions.

Through application of advanced imaging techniques, single-particle cryogenic electron microscopy (cryo-EM; Frank 2006; 2016; 2017) allows these macromolecules to be individually visualized after rapid freezing in vitreous ice at a rate that is assumed to be faster than the overall reconfiguration time of the system (Whitford et al., 2011). As a result, the ensemble of molecules closely approximates the thermal-equilibrium distribution of states immediately prior to being frozen. Cryo-EM aims to capture the activity of the macromolecule in its complete form, encompassing its continuum of accessible states.

The depth of information captured by cryo-EM has inspired numerous data-analytic approaches that aim to systematically uncover these ensemble-characteristics. The algorithms underlying the approach by Dashti et al. (2014) and later developments (Dashti et al., 2020 and Mashayekhi 2020), summarily referred to as *ManifoldEM*, are one such approach. ManifoldEM uses geometric machine-learning to identify the set of leading conformational motions best able to describe the function of a molecular machine. It is based on the premise that, for a sufficiently large set of snapshots obtained by single-particle cryo-EM, even energetically unfavored states of a molecule are observed. As a consequence, the snapshots – by virtue of their similarity relationships – form a quasi-continuum in high-dimensional space. Through manifold embedding, the data are represented in a minimal low-dimensional space where coordinate axes express modes of the conformational motions in a way that has to be discovered on a case-to-case basis. In the original paper (Dashti et al., 2014), these modes were termed "reaction coordinates," a term we wish to avoid as it has different connotations in other fields. Instead, following the terminology of Dashti et al. (2020), we will use "conformational coordinates" (CCs, for short) throughout this document.

Importantly, the number of sightings of a molecule in a particular state can be interpreted, via the Boltzmann relationship, as a measure of free energy (Fischer et al., 2010). This transformation adds probabilities to this space, giving the thermodynamic likelihood of a hop from any one state to any of its immediate neighbors. The global geometry of the energy landscape characterizes the molecular machine's navigational probabilities, with deep wells representing distinct regions of conformational states and mountainous regions constraining the transitions between them (Seitz and Frank, 2020). Further, since specific sequences of conformations give rise to biomolecular function, this descriptive mapping also identifies the molecular machine's functional dynamics. Through ManifoldEM, the potential now exists to create the conformational free-energy landscape for any molecular machine capable of being visualized by cryo-EM. Results from previous ManifoldEM studies on biological systems – including the ribosome (Dashti et al., 2014), ryanodine receptor (Dashti et al., 2020) and SARS-CoV-2 spike protein (Sztain et al., 2021) – have proven its viability and its potential to provide new information on the functional dynamics of biomolecules.

1.2 ManifoldEM Software Platforms

The original ManifoldEM methodology (Dashti et al., 2014) was implemented using Matlab code, and has recently been made available for Matlab users (Mashayekhi, 2020). The ManifoldEM Python Beta release mirrors an earlier (2019) 1D version of the Matlab code, except for a number of additional enhancements to be elaborated on below. Importantly, in this Beta release, only the generation of 1D energy paths have been made available. It is a work in progress to extend this software package to incorporate 2D energy landscapes as done in the current Matlab package (Mashayekhi, 2020). In addition, it is our plan for future ManifoldEM Python distributions to incorporate an alternative method – *ESPER: Embedded Subspace Partitioning and Eigenfunction Realignment* (Seitz et al., 2021) – able to combine with this current framework with potential to enhance the quality of its final outputs. There are also several limitations to the current ManifoldEM method that have been outlined by Mashayekhi (2020) and Seitz et al. (2021) – and detailed later in Appendix E – which we believe ESPER is able to circumvent. As a final note, as the more recent

version of the Matlab code has now been published as a separate, actively-managed branch (Mashayekhi, 2020), there is a future possibility of increasingly different, distinct features arising in the Matlab and Python versions.

The Python code comprises two features not contained in the original Matlab code: (1) an implementation of an automated angular propagation algorithm (Maji et al., 2020); and (2) an advanced graphic user interface (GUI) that integrates all Python code, communicates with all relevant files and facilitates the execution of essential operations, while providing informative visualization of important intermediate and final outputs. A few words about the importance of the GUI in steering and controlling the ManifoldEM analysis. Many advanced software systems now employed in cryo-EM are of the "black box" type, allowing only the specification of a command stream without feedback to the user, and without providing an intuition about the way parameter choices affect the outcome (Maji and Frank, 2021). In this they sharply differ from interactive modular software systems that popularized early research in single-particle cryo-EM (Frank et al., 1996; van Heel et al., 1996) and offered instant feedback. The diversity in the nature of the input data and in the kinds of questions asked in the ManifoldEM approach make the black box-type of user control difficult to sustain even by experts, and virtually impossible in the hands of non-expert users. The GUI presented here, by providing instant feedback on the impact of every parameter choice, puts the user firmly in the driver's seat, allowing them to steer the processing in the desired direction.

1.3 ManifoldEM Alpha Release

Internal testing and debugging of code was conducted during the process of translating Matlab code into Python and integration with GUI. More recently, a workflow for producing physically plausible synthetic data was created (Seitz et al., 2019) and implemented for testing the fidelity of all modules with heightened precision. By means of this flexible tool, the need for many of our previously-mentioned innovations was first encountered and answered. In order to expand our awareness of potential problems in software, performance and interface, we organized and conducted an Alpha version release of the ManifoldEM Python suite, with scope limited to acquisition of 1D energy landscape. All code was published on a private GitHub repository with detailed documentation provided on installation, initiation and overall use of the ManifoldEM GUI. The length of our alpha trial spanned approximately eight months, beginning in February and ending by late August, 2019.

Our Alpha user group encompassed 10 individuals, comprising scientists and engineers from various (cryo-EM related) fields. Extensive communications with these users were conducted by our team via email or private GitHub forum to provide guidance on operations and errors encountered. Alpha users were specifically instructed to test the software using their own or others' published online cryo-EM data sets. Both options were exercised, and as these users worked with a variety of operating systems and hardware, we encountered a unique range of situations and unique sets of problems to explore. This experience made us aware of shortcomings in documentation of workflow, helped guide our team towards optimizing software performance and provided

opportunities to enhance useability through the user manual and tutorial now included in this release. We hope this Beta release will likewise provide our team with useful feedback for improvement, achievable now from a wider and more diverse audience.

2 Installation

We next detail the steps required to install the ManifoldEM Python 3 environment, which uses packages required for visualization (frontend) and calculations (backend). The GUI is programmed using PyQt5 and TraitsUI, with data visualizations achieved via Mayavi (3D) and Matplotlib (2D). The majority of backend calculations are performed using NumPy. We also note that this Beta release has only been thoroughly tested on Linux and MacOS operating systems.

2.1 Getting Started

We recommend using a unique directory for each cryo-EM data set you want to analyze (hereby referred to as the *project directory*). The project directory can be downloaded from the GitHub ManifoldEM_Python master branch via the `clone or download` button near the top of the main page. Users can elect to either (1) download a `.zip` file and move it to their directory of choice – unzipping the package therein – or (2) navigate to their directory of choice in the command line interface (CLI) and perform the action: `git clone <link>`, where `<link>` is the GitHub-provided URL link (sans brackets). In either case, the ManifoldEM project directory will be created at this location and contain all the files needed to run the program.

Each ManifoldEM project directory should come equipped with: (1) a modules folder where all backend algorithms are stored; (2) a GUI file for running the user interface; (3) an icons folder for GUI graphics; (4) a copy of this manual; and (5) licensing information. You may find it convenient to store your relevant cryo-EM input files within this newly created project directory. The root folder name can be initially renamed to uniquely correspond to your project; however, it is imperative that this name is not altered after a new project has been initiated, and that the core files within the project directory are not edited or moved.

2.2 Installing the Environment

Before initializing the GUI, first install the latest version of Anaconda for Python 3 from https://www.anaconda.com/download/, which is used to run the Python code and all dependencies. Once installed, an Anaconda environment must be generated (which downloads and stores the libraries needed within each script). Navigate to your project directory via the command line. In CLI, first enter the command `conda create -n ManifoldEM python=3`, and then activate the created environment via `conda activate ManifoldEM`.

Next, install the following libraries in the order they are listed:

```
pip install numpy
pip install mayavi
pip install PyQt5
pip3 install --user psutil
pip install matplotlib
pip install scipy
pip3 install -U scikit-learn scipy matplotlib
pip install pandas
pip install mrcfile
pip install opencv-python-headless
pip install opencv-contrib-python
pip install mpi4py
pip install h5py
pip install imageio
```

If any other problems emerge during installation, proceed to Appendix A of this manual. Once the Anaconda environment is installed, it must be initiated each time before ManifoldEM is run via the command: `conda activate ManifoldEM`

When you are done using the program, always exit the environment via: `conda deactivate`

Now that the ManifoldEM environment is installed and sourced in your current terminal window, we can launch the ManifoldEM Python GUI. The GUI always needs to be launched from the desired project directory. Once inside the project directory, launch the GUI via:
`python ManifoldEM_GUI.py`

3 Imports Tab

Upon opening the ManifoldEM Python GUI, you will be presented with the option to start a new project or resume an existing one. If this wasn't your first time running the GUI, you could resume progress at this point on a previous project by selecting that project's parameters `.pkl` file.

After selecting to start a new project, you will land on the first tab of the GUI (the *Import* tab), where a number of fields are present requiring specific inputs. In order, these fields are: *Average Volume*; *Alignment File*; *Image Stack*; *Mask Volume*; *Project Name*; *Pixel Size*; *Resolution*; *Object Diameter* and *Aperture Index*. As well, two non-editable fields exist for *Shannon Angle* and *Angle Width*. We will next go through each of these inputs in turn.

(As a note for those unfamiliar with cryo-EM terminology, the use of "volume" above is unique to the cryo-EM community, and is shorthand for a "3D reconstruction" or, more technically, a "3D Coulomb potential map". Throughout this document, we will use "volume" to designate a 3D Coulomb potential map resulting from 3D reconstruction in cryo-EM).

3.1 Average Volume

For this entry, browse for your molecule's Coulomb potential map (`.mrc`). For the RyR1 data set, search for the file `RyR1_AvgVol_Binned.mrc` in the `\demo` directory of the ManifoldEM Python repository. If you are running your own data set, this volume can be obtained by performing 3D Auto-Refine on your alignment file in RELION. This average volume file will only be used to help you navigate key aspects of your molecule throughout the ManifoldEM GUI. It has no other purpose in the workflow.

3.2 Alignment File

For this entry, browse for your molecule's alignment file (`.star`), which links each of the 2D images in the image stack to their corresponding orientational angles and related microscopy parameters. This file is the product of orientational recovery via RELION as obtained either prior to 3D classification or after combining a subset of classes from 3D classification. Please see the *Resolution* section for guidelines on achieving optimal results. If running with the demo RyR1 data set, search for the file `RyR1GCs_clustRem.star`. ManifoldEM requires (at minimum) the following parameters within the alignment file: *Image Name*; *Angle Rot*; *Angle Tilt*; *Angle Psi*; *Origin X*; *Origin Y*; *Defocus U*; *Defocus V*; *Voltage* and *Spherical Aberration*. To note, ManifoldEM is not currently set up to calculate elliptical defocus; instead, it treats all cases of defocus as spherical. As well, although the software is set up to handle image recentering, if your original micrographs are available, we recommend recentering before ManifoldEM (and thus also setting *Origin X* and *Origin Y* values in the alignment file to zero) as to avoid introduction of padding artifacts that could lower the fidelity of the distance matrix.

We also note that ManifoldEM accepts both former and current (version-3.1) RELION formats. The script `read_alignfile.py` automates this decision based on the presence of "data_optics" in the header of the alignment file. Please consult the demo file `RyR1GCs_clustRem.star` as reference for pre-3.1 formatting. If using an alternative package (e.g., cryoSPARC), alignment files will need to be converted appropriately. For the example of using cryoSPARC, tools such as PyEM can be used to convert to RELION.

3.3 Image Stack

For this entry, browse for your molecule's image stack (`.mrcs`), which is the set of all individual molecular images obtained from particle picking. If running with the demo RyR1 data set, search for the file `RyR1GCs_clustRem.mrcs`. We suggest that all images are unbinned and standardized (with average density in the background approximately 0 and standard deviation in noise approximately 1). If you have multiple image stack files spread out across one or many folders, we also require they first be joined into one singular stack for import into ManifoldEM. This can be done using the image stacks' corresponding alignment file via the RELION command:

```
relion_preprocess --operate_on FOO.star --operate_out BAR
```

This operation will create a new (possibly smaller) alignment file and image stack containing only those images referenced in the original alignment file.

3.4 Mask Volume

This entry is optional and should be included if you wish to mask out a specific region of your molecule for processing in ManifoldEM. If running with the demo RyR1 data set, you can leave this entry blank. Using this volumetric mask, all exterior voxels/pixels will be ignored during all future computations (i.e., *Distances* and *Optical Flow*, which will be discussed later in this manual).

Volume Masks must be created external to ManifoldEM. While several methods exist, here we detail one such workflow using Chimera and RELION. Assuming you have access to your macromolecule's structural information (in the form of 3D atomic coordinates from the PDB), Chimera's `molmap` command (along with a given input resolution; e.g., `20`) can be used, followed by resampling of that output volume (`#1`) onto the original coordinates. For example, this last step can be achieved by importing your class average `#0` into the scene and translating the new volume `#1` to match its position, then running `vop resample #1 onGrid #0` to produce a resampled volume (`#2`). Next, alter the isosurface level of the volume `#2` in Chimera as needed and record the final number. After saving this volume to file, `relion_mask_create` can be used (making sure to set the threshold `--ini_threshold` in correspondence with your preferred isosurface level from Chimera) to create an inclusion mask.

3.5 Project Name

This entry is optional and can be used for supplying names for different projects within the same project directory. If no name is provided, the current date and time (taken when the project was initialized) will be used. This project name will be used in the titles of both the `outputs_<project name>` folder (containing all backend calculations) and `params_<project name>` file (containing all user-defined parameters). If you choose a project name that is already being used within the same project directory, you will be asked to either choose a different name or overwrite the previous outputs folder and parameters file before proceeding to the next tab.

3.6 Pixel Size

This parameter defines the pixel size (Å/pixel) of the camera used to obtain your cryo-EM images. This value can be found within your alignment file (`rlnPixelSize`), or if not present there explicitly, can be obtained by dividing the value for `rlnDetectorPixelSize` by `rlnMagnification`. For example, if your STAR alignment file shows a *Detector Pixel Size* of 5 μm and *Magnification* of 31000, your *Pixel Size* can be obtained via: 5e-6 / 31000 = 1.6129e-10.

If running with the demo RyR1 data set, set this value to 1.255 Å. As a note on RyR1, the published *Pixel Size* actually deviates from the value obtained via the above calculation due to an additional calibration technique. As a rule of thumb, if using a previously published data set, always make sure to use the final value as listed in the publication itself.

3.7 Resolution

This parameter defines the resolvability in the Coulomb potential map of your molecule obtained from Fourier Shell Correlation. If running with the sample RyR1 data set, set this value to 5 Å. If using your own data set, the resolution can be obtained by running RELION 3D Auto-refine on your alignment file. After doing so, navigate to the `run.out` file from the final iteration; near the bottom of this file, you will find: `Auto-refine: + Final resolution (without masking) is: <float>`. It is important to note that pursuing the highest resolution possible can actually be counterproductive in determining the conformational continuum by ManifoldEM, as a tradeoff exists between spatial resolution of a volume (representing an average of some limited number of states) and differentiation of states (i.e., resolution in state space) in the molecule's quasi-continuum. Therefore, preprocessing techniques (such as data cleaning and removal of low-occupancy class averages) should be as careful as possible to preserve the widest spectrum of your molecule's states. Please see Appendix C for more information on preprocessing.

3.8 Object Diameter

This parameter describes the maximum width of your protein structure; and should be taken to approximate the maximum width of your molecule across all obtained projection directions and

conformations. If unknown, this distance can be approximated using Chimera. In Chimera, open the 3D Auto-refine MRC volume, navigate to the *Tools* > *Volume Data* > *Volume Tracer* window, and place two data points on the most diametrically opposed voxels in your structure (with controls determined via the *Place Markers* setting of that subwindow). Once these two markers are placed, *Ctrl*-click the first marker, then *Ctrl+Shift*-doubleclick the second marker. Finally, choose the *Show Distance* popup when it appears. If running with the sample RyR1 data set, you can set this value to 360 Å as recommended in Mashayekhi (2020).

3.9 Aperture Index

This parameter is an integer describing the aperture size in terms of the Shannon angle. If running with the sample RyR1 data set, set the aperture index to 4. We recommend always starting with an aperture index of 1. After all other inputs have been entered on the *Import* tab, the effects of this value can be determined on the next tab (*Distribution*). We'll describe how to measure the goodness of each aperture index in our discussion on *Tessellation Thresholds* in the next section. If you find that an aperture index of 1 is unsuitable by the standards described there, you can return to the first tab and increase its value to 2, repeating this process until an optimal value is obtained.

3.10 Shannon Angle

The Shannon angle is used to calculate the orientation bin size. This value will automatically re-adjust as the other user inputs are altered. It is defined via:
Shannon angle = *resolution* / *object diameter*

3.11 Angular Aperture Width

This parameter represents the width of the aperture on S^2 (in radians). Like the *Shannon angle*, this value will automatically re-adjust as the other user inputs are altered. It is defined via:
angle width = *aperture index* × *Shannon angle*.

Once all inputs have been entered (sans optional entries: *Mask Volume* and *Project Name*), click the *View Orientation Distribution* button at the bottom of the window to proceed to the *Distribution* tab.

4 Distribution Tab

The user alignment file contains information on the rotational orientations of each snapshot in the ensemble. These images are naturally distributed across accessible orientations over an angular space known as the two-sphere (S^2). ManifoldEM bins images within local clusters on S^2 defined by the boundaries of tessellated regions (a mosaic pattern of many virtually identical shapes fitted together; Lovisolo et al., 2001). The size of the shapes used within this spherical tessellation is determined by the *Angle Width* calculated on the first tab. Each tessellated region is given a unique set of orientational angles defined by the average of the angular location of all images falling within its boundaries.

The location of each of these centers on S^2 are called *Projection Directions* (PDs), and represent an average view of your molecule as seen from a collection of unique viewing angles. This allows the group of images residing within the boundaries of each PD to be analyzed as sets independently from all others. In this way, the inner conformational mechanics of the molecular machine are isolated from the angles in which the molecular machine can be viewed in space. Naturally, as the *Angle Width* increases, the total number of PDs will decrease while the number of images contained in each of those PDs will increase.

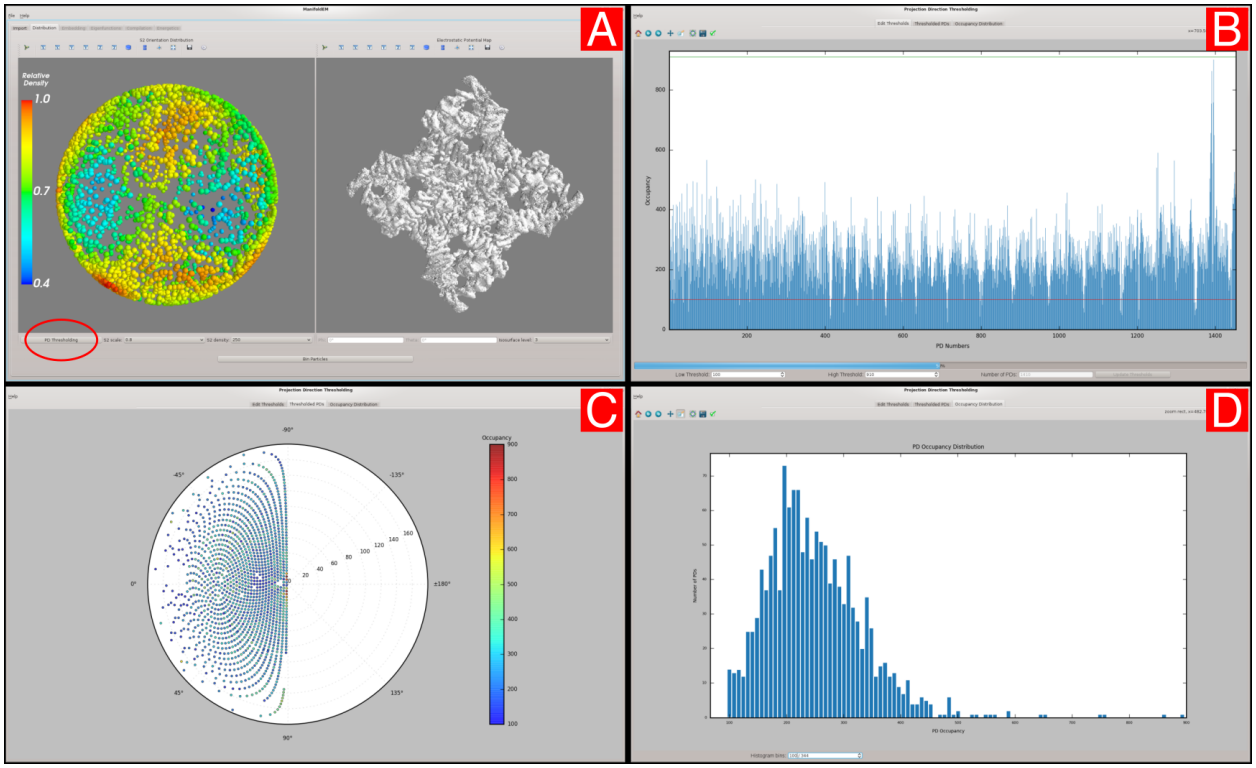

Figure 1: Distributions for RyR1 (full −ligand data set) as visualized on the *Distribution* tab: [A] *Distribution* tab; [B] *Edit Thresholds*; [C] *Thresholded PDs*; [D] *Occupancy Distribution*. To note, subwindows [B], [C] and [D] are accessed via the encircled *PD Thresholding* button on the main *Distribution* tab. If you are using the demo data set, the available PDs will form a great circle in angular space.

4.1 Orientation Navigation

Upon landing on the *Distribution* tab (Figure 1-A), you will see two figures that allow you to view your molecule's S^2 *Orientation Distribution* (on the left) in tandem with its corresponding *Electrostatic Potential Map* (on the right). Both figures are synced such that navigating the Mayavi camera within either figure will automatically update the view of the other. The S^2 *Orientation Distribution* figure plots the occupancy of the projections mapped across S^2, with corresponding heatmap defining the relative spatial density of projections. You can change the density of points shown via the S^2 *Density* value (e.g., 5 means that only every other 5^{th} image will be plotted as a point in these coordinates). Be careful not to select more points to plot than your computer can handle; by default, ManifoldEM chooses a very conservative value based on the size of your image stack. The *Electrostatic Potential Map* is a depiction of the volume file you imported on the previous tab. You can cycle through its contour depth via the *Isosurface Level* control. In the event that these two objects are initially plotted with disproportionate scales, you can also change the relative scale of these two figures via the S^2 *Scale* value. In addition, the Mayavi icon can be clicked above each figure to open a dialog housing expansive visualization options. The most recent settings chosen for S^2 *Scale* and *Isosurface Level* will also be applied to the equivalent figure on the *Eigenvectors* tab.

As you move the camera in either scene, notice that the current *phi* and *theta* value is updated in the entries below. These are taken as the combination of Euler coordinates from which you are viewing your objects. A guide for understanding the camera controls can be found in Appendix B of this manual. To fully understand how your data has been tessellated, we'll need to next explore the *PD Thresholding* subwindow, accessed via the corresponding button in the lower left-hand corner of the *Distribution* tab.

4.2 Tessellation Thresholds

There are three tabs within the *Projection Direction Thresholding* subwindow: *Edit Thresholds* (Figure 1-B), *Thresholded PDs* (Figure 1-C), and *Occupancy Distribution* (Figure 1-D).

On the *Edit Thresholds* tab, the bar chart shows the number of images captured within the boundaries of each PD for the given *Angle Width*, with the *PD Number* plotted on the x-axis: labelling each PD based on an arbitrary assignment of integers. This window also has two parameters: *Low Threshold* and *High Threshold*. As these values are changed, the red and green horizontal lines in the plot will shift their vertical position respectively. If a PD has fewer images than the number specified by the *Low Threshold* parameter (red line), that PD will be ignored across all future computations. The value shown in the *Number of PDs* display will also be updated to reflect this change. If a PD has more images than the number (n) specified by the *High Threshold* parameter, only the first n images under this threshold will be used for that PD. To finalize new *Low* and *High Thresholds*, make sure to click the *Update Thresholds* button at the bottom of this tab before exiting the subwindow. If you're using the demo RyR1 data set, the default low and high thresholds can be used, resulting in 53 PDs.

The next tab over on the *PD Thresholding* subwindow (*Thresholded PDs*, Figure 1-C) shows the number of remaining PDs after thresholding. These are plotted with polar coordinates, displaying *phi* values on the perimeter-subdivisions and *theta* values on the radial-subdivisions. The occupancy of each remaining PD can be seen via the colorbar on the right. The third tab (*Occupancy Distribution*, Figure 1-D) displays a histogram showing the distribution of PD occupancies (the number of images in each PD) across all PDs. The number of histogram bins can be altered via the entry at the bottom to expand on this characterization. Using these three tools, you should be able to make an assessment on the overall goodness of the *Angle Width* calculated on the *Import* tab (and thus the variable *Aperture Index* you supplied). You want to find the optimal *Aperture Index* such that the tessellation provides the most coverage across the S^2 (as seen on the *Thresholded PDs* tab) while also having a sufficient number of images in each PD (as seen on the *Occupancy Distribution* tab).

As this is a very qualitative assessment, we note an additional option for those still unsure. It is possible to first perform a test-run by increasing the low threshold value such that only a handful (5-10) PDs are selected, and then decreasing the high threshold to the average value of images seen across all PDs. Next, proceed through the *Embedding* tab (as described in the next section) with this small sample and assess the quality of your conformational motions on the *Eigenvectors* tab. If the motions present are too much obscured by noise or if too few motions are present per PD, you'll want to consider choosing a larger *Aperture Index* for your data set. In contrast, choosing an *Aperture Index* that is too large may result in prominent CCs exhibiting rigid body rotations of your macromolecule across the S^2. Once you have found the optimal *Aperture Index* for your needs, make sure to create a fresh project where it is entered, while re-assessing your low and high thresholds to instead calculate the full set of your best PDs.

If you try to move past tab 2, the GUI will provide you with a warning message. Upon choosing to proceed, all of these previously established user-parameters will be locked in permanently for the remainder of your project.

5 Embedding Tab

Within each isolated PD, embedding techniques are applied across the collection of corresponding images to discover the latent conformational mechanics of the molecular machine (as seen from that PD). These steps are performed in sequence on the *Embedding* tab, and are laid out into four modules: *Distance Calculation*, *Embedding*, *Spectral Analysis*, and *Compile 2D Movies*.

5.1 Embedding Parameters

Before initiating the first module (via the *Distance Calculation* button), take note of the three entry fields at the top of this tab: *Processors*, *Eigenvectors*, and *Dimensions*.

5.1.1 Processors

The *Processors* entry dictates the number of processors (corresponding to the number of PDs) your computer will run in parallel during the proceeding steps. The maximum number is determined by your workstation specs. This value should be set before pressing the *Distance Calculation* button below, and cannot be changed again until all processes are complete (or if the project is quit, and then resumed). As a note, if you ever need to debug an error that occurs, always re-run with *Processors* set to 1, which will enter into single-processing mode. In this mode, command line error messages are unobstructed from multiprocessing packages, providing the best diagnosis for your problem. If you're encountering performance problems (slowdowns or crashes), you may want to consider running fewer processors.

5.1.2 Eigenvectors

The *Eigenvectors* entry is used to set the number of leading eigenvectors corresponding to the diffusion maps embedding (discussed below), which are used in NLSA across all PDs. While a total of 15 eigenvectors are used by default throughout all backend computations, the *Eigenvectors* entry determines the number of leading eigenvectors from that set (up to a maximum of 8) for which a NLSA will be performed. Importantly, only members from this set will be selectable as potential conformational coordinates on the subsequent tabs, and once this decision is made, it cannot be reversed. We recommend the maximum (8) if computational resources and time are plentiful. If performing a test run on a subset of PDs, a much lower number (e.g., 1 to 3) is sufficient.

5.1.3 Dimensions

The *Dimensions* value defines the number of dimensions to be used in defining the conformational coordinates (termed *Conformational Coordinates* or *CCs*) of the energy landscape. As an important note, this value has been restricted to 1D for the Beta release.

With these three parameters filled, it's time to start computing. The modules on this page can take considerable time to compute (especially if a large number of *Eigenvectors* are chosen). If your progress is interrupted at any time or if you need to exit the program, you can always resume from where you last left off upon re-opening the GUI.

5.2 Distance Calculation

The first step in the manifold embedding pipeline is the construction of the distances graph (initiated upon clicking the *Distance Calculation* button), in which the similarity of each image to the other images in each PD is calculated.

5.3 Embedding

The next module (initiated via the *Embedding* button) uses the previous distance calculations to create nonlinear conformational manifolds via the *diffusion maps* method (Coifman et al., 2006). This embedding automatically yields orthogonal coordinates (eigenvectors) ranked according to eigenvalue, with each coordinate assumed to describe a set of concerted changes.

5.4 Spectral Analysis

To reveal the nature of changes associated with each individual coordinate after the initial embedding, *Nonlinear Laplacian Spectral Analysis* (NLSA; Giannakis, 2012) is used. During the performance of NLSA, the original cryo-EM images are concatenated along one of the leading k eigenvectors to produce a spatial series of so-called "supervectors" (Dashti et al., 2014). Nonlinear SVD (via NLSA) is then used to extract characteristic NLSA images (*topos*) and their evolutions (*chronos*) from these supervectors. Each topo/chrono pair constitutes an element of a biorthogonal decomposition of the conformational changes along the given eigenvector. Noise-reduced snapshots can be reconstructed from the topo/chrono pairs with significant (above-noise) singular values and embedded to obtain the manifold characteristic of the conformational changes along the selected line. This embedding results in a new set of eigenvectors in a different space, to high accuracy forming a 1-dimensional manifold with known eigenfunctions $\{\cos(k\pi\tau) \mid k \in \mathbb{Z}^+\}$ parameterized by a conformational parameter τ. This process enables the estimation of a density of points as a function of τ together with an ordered sequence of 2D NLSA images. These 2D images are arranged to form a 2D NLSA movie, designed to represent the conformational signal corresponding to the eigenvector chosen from the initially-embedded manifold. In total, NLSA is performed for each of the leading k eigenvectors independently, such that k 2D NLSA movies are constructed for each PD.

Supervised identification of "meaningful" conformational information (i.e., the CCs) among these k 2D NLSA movies is next required,with subsequent steps aimed at then connecting these CCs across all PDs. Once the NLSA movies have been computed via the *Compile 2D Movies* module, you can navigate to the *Eigenvectors* tab via the *View Eigenvectors* button at the bottom of the page. As an important note, in the event that the *Spectral Analysis* module stalls (i.e., a relatively prolonged

period of time has elapsed since the previous file was written), counter-measures may need to be explored. For more information, please see Appendix E for a description of bypassing stalled PDs.

6 Eigenvectors Tab

You will find that the *Eigenvectors* tab is segmented into 4 main parts (Figure 2), these are: (A) *PD Selection*; (B) *PD Eigenvectors*; (C) *Anchor Assignment*; (D) *Confirm Conformational Coordinates*.

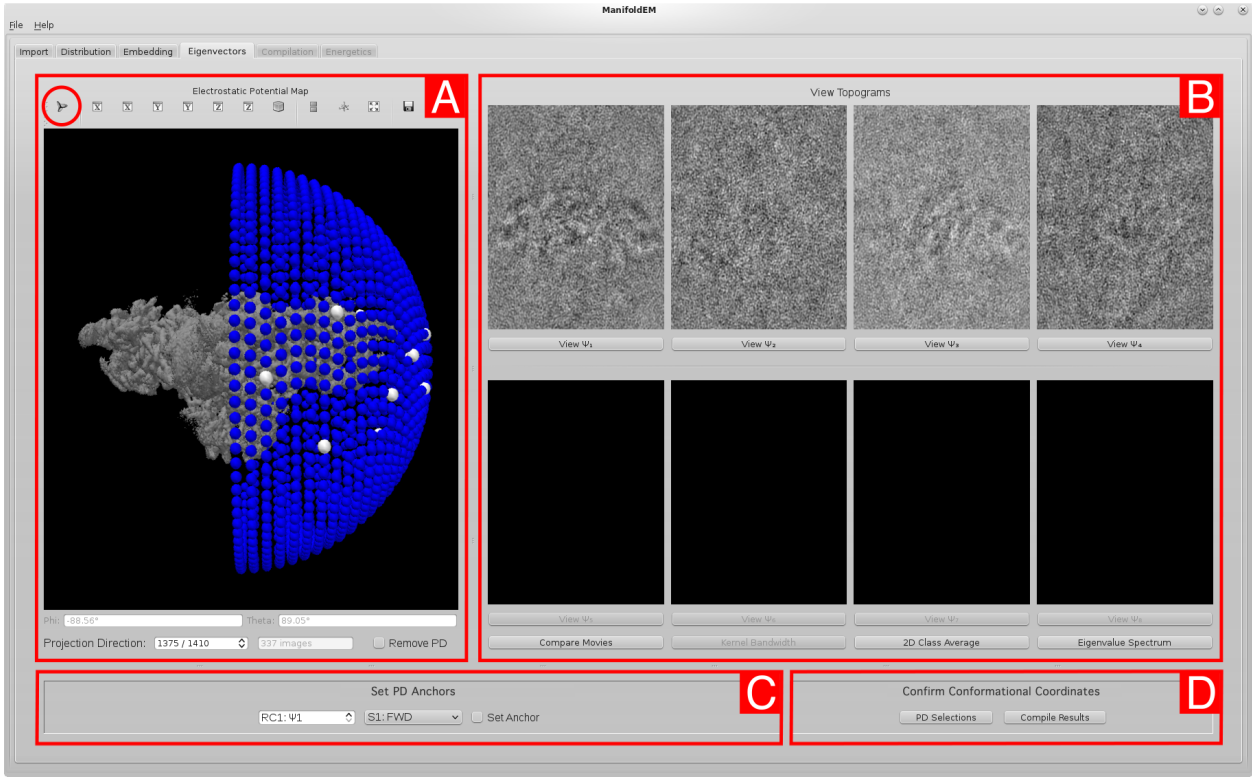

Figure 2: Outputs of the *Embedding* tab for RyR1 (full −ligand data set) as visualized on the *Eigenvectors* tab. For changing all volume representation settings (including isosurface levels), click the encircled Mayavi icon. The black boxes in subsection [B] are a result of choosing only four *eigenvectors* on the previous tab. Also take note of the two subdividing lines separating these regions (first between [A, B] and second between [AB, CD]), which can be dragged with the mouse to redistribute window spacing between *Eigenvectors* tab subsections as needed.

6.1 PD Selection

In the figure window entitled *Electrostatic Potential Map*, you will find a series of colored nodes encircling the input volume. Each node represents a unique PD from the set of all PDs obtained after thresholding. By default, the page will open on the first PD, such that all of the initial information on the *Eigenvectors* tab relates to this PD's characteristics. The colors of these nodes signify groupings of *Connected Components*: clusters of PDs that were deemed in close enough proximity to reliably pass the information on conformational motion between them during *Belief Propagation* (discussed in a later section). For example, if you have two clusters of PDs separated by a relatively large

distance in angular space (likely due to preferred orientations in experiment), two distinct colors will be used for each cluster.

As you change the Mayavi camera angle in this subwindow (Figure 2-A), you can move from one PD to the next. Releasing the mouse while hovering over a new location in the subwindow will immediately snap the view to the PD closest to your current hover position, updating the entire *Eigenvectors* tab in turn to correspond to this new PD's characteristics. You can also elect to travel directly to a specific PD via the *Projection Direction* entry (which reads as: *PD Number / Total Number of PDs* seen at the bottom of Figure 2-A). To be specific, whenever a new PD is visited, you will see the following entries update to correspond to this PD's attributes: the *phi* and *theta* values below the figure, the *Projection Direction* number, the number of images in the current PD, all anchor information, *2D Class Average* graph, *Eigenvalue Spectrum* graph, all images within the *View Topos* subsection of the *Eigenvectors* tab, and all graphs accessed via buttons therein.

The figure itself will also update when either the *Remove PD* or *Set Anchor* checkboxes are selected, turning the current node to either black or white, respectively. If the box for *Remove PD* is checked for a given PD (to be done only if the information in that PD is deemed undesirable), ManifoldEM is instructed to ignore it in all future computations. Anchor PDs play a much larger role, and will be discussed in greater detail in the forthcoming sections.

6.2 PD Eigenvectors

When viewing a PD on the *Eigenvectors* tab, all of its conformational information from the previous calculations is isolated for detailed analysis. The eight windows in Figure 2-B present the deviation of the data from the mean (Topo) along the first i eigenvectors ($\Psi_1, \ldots, \Psi_i$); with i defined via the *Eigenvectors* setting on the *Embedding* tab . The properties of each of the PD's eigenvectors (Ψ_i) can be explored under the *View Topos* heading by clicking the corresponding *View* Ψ_i button underneath that specific window. Click the *View* Ψ_1 button (seen in Figure 2-B) to open the analysis subwindow for the current PD's most prominent conformational motion. Inside of each *View* Ψ_i subwindow, you will find a number of tabs: *Movie Player; 2D Embedding; 3D Embedding; Chronos; Psi Analysis; Tau Analysis.*

6.2.1 Movie Player

The NLSA movie player displays the NLSA frames in sequential order from frame 1 to frame 50. Each of these frames can be thought of as depicting an individual state, and the collection of frames describes the conformational motion along a given eigenvector. Along with standard playback controls, the movie can be scrubbed through via the slider at the bottom of the subwindow.

6.2.2 2D Embedding

The *2D Embedding* tab projects the PD's diffusion map embedding onto a two-dimensional plane. The first dimension is set by the currently chosen eigenvector, while the second dimension is set by

the eigenvector having the next highest eigenvalue. By clicking anywhere on this plot, a red cross will appear. Clicking again at a different location will spawn a second red cross which is immediately connected to the first by a gray line. This tool can be used to draw shapes in the figure, such as to enclose outlier clusters (with each point in the cluster representing an image). Once more than two red crosses have been added, you can close your shape by pressing the *Connect Path* button at the bottom of the page. Once the shape is closed, you can elect to view an average of all of the images within that enclosed region via the *View Cluster* button, or to remove the cluster entirely via the *Remove Cluster* button. At any time, you can also reset the shape by pressing the *Reset Plot* button.

Once a cluster has been removed, you must press the *Update Manifold* button for changes to take place. This operation will tell the backend algorithms to recompute the manifold analysis steps using only those images remaining after your removal. Upon completion of the cluster removal, the subwindow will close, signifying that all eigenvector plots for the current PD have been updated. At any time, you can navigate back to the *2D Embedding* screen and revert your changes via the *Revert Manifold* button.

6.2.3 3D Embedding

The *3D Embedding* plot is a visualization tool for viewing the diffusion map embedding in combinations of three coordinates. You can use the *X*-axis, *Y*-axis, and *Z*-axis entries at the bottom of the screen to choose which combination of eigenvectors you'd like to use as coordinates. In addition, you can rotate the plot in this selected 3D subspace to better understand the shape of your data. This tool is especially useful for identifying candidate outlier clusters for removal.

6.2.4 Chronos

In this window, the *chronos* coming from *Spectral Analysis* are plotted. By default, only the first two modes are retained to extract the NLSA images. In a later version of ManifoldEM, users will be given the option to re-embed each manifold by selecting a new combination of these modes based on qualitative assessment. For more information on *chronos*, see the supplementary material in Dashti et al. (2014).

6.2.5 Psi Analysis

As mentioned in the *Spectral Analysis* section, after embedding the noise-reduced snapshots (reconstructed images), the resulting 1-manifold should have a parabolic structure. If a 1-manifold is not parabolic, the PD's corresponding *Diffusion Map* may be inadequate either due to a lack of snapshots from experiment, an unfavorable distribution of those snapshots within the corresponding tessellated region of S^2, or because of the presence of outliers (appearing as separate data clouds in the *Diffusion Map*). In the latter case, see the *2D Embedding* section on how to re-embed the *Diffusion Map* to possibly recover a parabolic 1-manifold via NLSA. However, if there are no easily identifiable divergent clusters in the *Diffusion Map* to remove, you may want to

consider removing the PD completely (see the forthcoming *Confirm Conformational Coordinates* section for more information on this process).

6.2.6 Tau Analysis

On the *Tau Analysis* tab, you'll find two figures. In the left figure, every NLSA image index in the PD is plotted in accordance with the NLSA state to which it has been assigned. The figure on the right provides a histogram of this *Tau Parameterization*, showing the overall NLSA image occupancy for each of the NLSA states. This information will eventually be propagated across all PDs for each user-defined eigenvector.

6.2.7 Eigenvalue Spectrum

Along with the data pertaining to each individual eigenvector, distributions relating to the bulk properties of all eigenvectors in each PD can also be viewed. Click the *Eigenvalue Spectrum* button to view the relative strength of the PD's eigenvectors (each representing an orthogonal conformational motion captured within the DM embedding). In this figure, the blue bars signify those eigenvectors that were calculated for detailed analysis (set via the *Eigenvectors* entry on the *Embedding* tab). All other eigenvectors will be demarcated with gray, and have black images displayed for their corresponding analysis in the *View Topos* GUI subsection on the main page (see Figure 2-B). The larger the eigenvalue (y-axis) is for each eigenvector, the more prominent the conformational motion along that eigenvector is relative to all others. Next, click the *2D Class Average* button to view an average of all images contained within the current PD.

6.2.8 Gaussian Kernel Bandwidth

Clicking the *Kernel Bandwidth* button will open a log-log plot of the sum of the elements of the pairwise similarity matrix as a function of the Gaussian kernel bandwidth (ε). The linear region of the hyperbolic tangent delineates the range of suitable epsilon values for the diffusion map embedding. Twice the slope at the inflection point provides an estimate of the *effective dimensionality* of the data (Ferguson et al., 2010). Visually, you should see a good fit to the hyperbolic tangent, while quantitatively, this goodness-of-fit should manifest in a R^2 value close to 1. We note that while the Gaussian kernel bandwidth is well estimated, the value for the effective dimensionality is unreliable. However, we include it here for completeness, and have provided more information on this discrepancy in Appendix E.

6.3 Anchor Assignment

After viewing the eigenvector information (especially the 2D NLSA movies) for several different PDs spread out across S^2, you should start to form a good idea of the types of conformational motions present in your data. The next step is to decide which one of these motions you would like to compile across all PDs to ultimately produce a corresponding *1D Energy Path* for that motion, along with a *NLSA Image Stack* and accompanying *NLSA Alignment File* for use in 3D reconstruction. This motion should preferably be both biologically relevant and also easily observable within one of the

available eigenvectors across the majority of your PDs. Eigenvectors containing this motion may also have a relatively high eigenvalue in each PD's *Eigenvalue Spectrum*, but, due to the changes in viewing directions, this is not always the case.

Once you have made your decision, go to the PD where this motion is the most easily identifiable. In order to tell ManifoldEM your choice, you'll need to use the tools within the *Set PD Anchors* section at the bottom of the *Eigenvectors* tab (Figure 2-C). In the *Conformational Coordinate 1* (CC1) entry box, put in the number corresponding to your motion's eigenvector within the current PD. In the next entry (S1, for *Sense 1*), you have the option to choose either *Forward* (FWD) or *Reverse* (REV). The *Sense* defines the directionality of your motion in each PD; you may have noticed that in some PDs, your motion is playing in reverse with respect to movies of that same motion in other PDs. For the first anchor, this choice is arbitrary and completely up to you. However, in each subsequent anchor you may choose, the *Sense* of its 2D NLSA movie must be consistently defined relative to all others. Once you have filled in these options for your first PD anchor, click the *Set Anchor* checkbox (Figure 2-C). You'll notice that the node representing your current PD in the figure above will update its color to white to signify this change.

In theory, you can hand-select every PD in this way, being careful to choose the correct eigenvector number and sense for your conformational motion in each PD until every node on your figure is colored white. We've even included a feature for aiding in such a task (within the *Compare Movies* subwindow) where you can directly compare any two NLSA movies side-by-side while altering these parameters as you see fit. However, in practice, such a workflow requires painstaking attention to detail and tremendous time, while also being significantly prone to human error (especially when dealing with hundreds or thousands of PDs).

Instead, we've attempted to optimize this procedure through a combination of *Optical Flow* and *Belief Propagation* (discussed in more detail within a later section) that approximately follow the same human-performed algorithm proposed above (Maji et al., 2020). For this automation strategy to work, only a handful of PDs are required in total. Importantly, we require a minimum of one anchor per *Connected Component*, but the more that can be accurately defined, the better. To be clear, you must make sure that the eigenvectors chosen as anchors are those of highest user certainty, since placing an erroneous anchor into these algorithms will most likely produce chaotic results.

If using the demo RyR1 dataset, however, it could be a helpful exercise to pick the 53 PDs present therein by hand. Since there are only a few dozen PDs to consider, this exercise should take about 20 minutes, while also reinforcing an understanding of essential concepts for new users seeking training. There are also a few PDs that should be removed. The following provides the decision process needed to assign one such anchor when using the RyR1 data set:

"Starting at a highly informative PD for the first anchor (where all motions are present and easily identifiable across all eigenvectors), which of its eigenvectors (1-8) represents the readily-identifiable 'wing' motion of RyR1; and is this motion playing (arbitrarily) FWD or REV within that eigenvector (as

seen in the 2D NLSA movie)? Next, is there another (preferably distant) PD where this same motion can also be easily identified across its set of eigenvectors, and is its NLSA movie playing FWD or REV with respect to the arbitrary Sense-assignment of the first anchor chosen?"

Our general workflow for assigning these anchors is to first check on the PDs with the highest occupancy via the *PD Occupancies* button within the *PD Selections* subsection on the *Eigenvectors* tab (Figure 2-D). For the RyR1 demo, search for the first PD in the ranked *PD Occupancies* list that offers a good side view of RyR1, and determine if there is a 2D NLSA movie showing the wings moving up/down with an accompanying "smooth" parabola in *Psi Analysis*. If there is more than one option showing this motion, pick the leading eigenvector. Next, arbitrarily define the directionality of motion (*sense*) as FWD; reserving REV for 2D NLSA movies playing in the opposite direction.

After setting this anchor information in the *Set PD Anchors* panel on the main *Eigenvectors* tab, it is ideal to next increase S^2 coverage by sporadically labelling a collection of spread out PDs with anchor information. However, this should only be done for PDs where user confidence of eigenvector/sense for the given CC is highest. If using the RyR1 demo data set with the suggested parameters, you will see that the PD nodes are grouped into two clusters (*Connected Components*) on S^2, with the nodes from each cluster visualized by red or blue coloring, respectively. When numerous connected components exist, at least one PD anchor must be defined in each cluster so that Belief Propagation can connect the conformational information across large empty regions on S^2. For the demo data set, we recommend defining three spatially-separated PD anchors in each connected component corresponding to the RyR1 wing-like motion. As a final note, during this assessment, it is highly recommended that users remove PD nodes that provide no meaningful conformational information. For the demo RyR1 data set, we identified and marked 7 PDs for removal using the GUI interface.

6.4 Confirm Conformational Coordinates

Once a sufficient number of PD anchors have been chosen, a list of all user PD selections can be accessed via the *PD Selections* button within the *Confirm Conformational Coordinates* subsection at the bottom of the *Eigenvector* tab (Figure 2-D) . In this subwindow, there are two tabs: *PD Editor* and *PD Viewer*.

The *PD Editor* tab allows you to view tables of all of your assignments for PD anchors and removals, as well as reset your current selections of each class independently. Moreover, this tab provides a way to save the currently selected *PD Anchors* and *PD Removals* as individual lists and load them back in whenever needed. It is important to note that these selections are automatically saved upon reaching the *Compilation* tab, but if you need to exit the program for any reason before all intended anchors have been chosen (and thus before pressing *Compile Results*), it is essential that you save your selections via these options. Finally, you can also view a sorted list of all PD occupancies as well as a list of PDs which have undergone manifold re-embedding (as described in the *2D Embedding* section above).

The *PD Editor* tab provides a polar-coordinate plot of all PDs according to their current user-defined class. PD anchors are shown as gray diamonds and PD removals as black × marks. All other PDs that are to-be-determined (TBD) by automation are displayed as colored dots corresponding to their *Connected Component* grouping. Once you are satisfied with your choice of PD anchors, removals and re-embeddings, click the *Compile Results* button at the bottom of the *Eigenvectors* tab to proceed.

7 Compilation Tab

You'll arrive next on the *Compilation* tab, where the conformational information from each individual PD is stitched together into one global identity. Much like the *Embedding* tab, you'll find a row of user-defined parameters at the top of the window (*Processors, Temperature* and *Export Optical Flow)* as well as a set of modules (*Find Conformational Coordinates* and *Energy Landscape)* for initiating the corresponding backend algorithms and gauging their progress.

7.1 Compilation Parameters

7.1.1 Processors

The *Processors* entry dictates the number of processors your computer will run in parallel during the proceeding steps. It will mirror the number set on the *Embedding* tab, but can be altered here as needed before proceeding with the final outputs.

7.1.2 Temperature

The value set in the *Temperature* entry should correspond to the pre-quenching temperature of the experiment immediately prior to rapid freezing. Specifically, it will be used in the Boltzmann relationship to convert image occupancies into energies.

7.1.3 Export Optical Flow

This parameter is completely optional, and if turned on, will export additional images of optical flow vectors to file during computation of the chosen conformational coordinate (Figure 3). As an important note, turning this option on will significantly increase computation time, and should only be used for investigating the underlying behavior of these outputs.

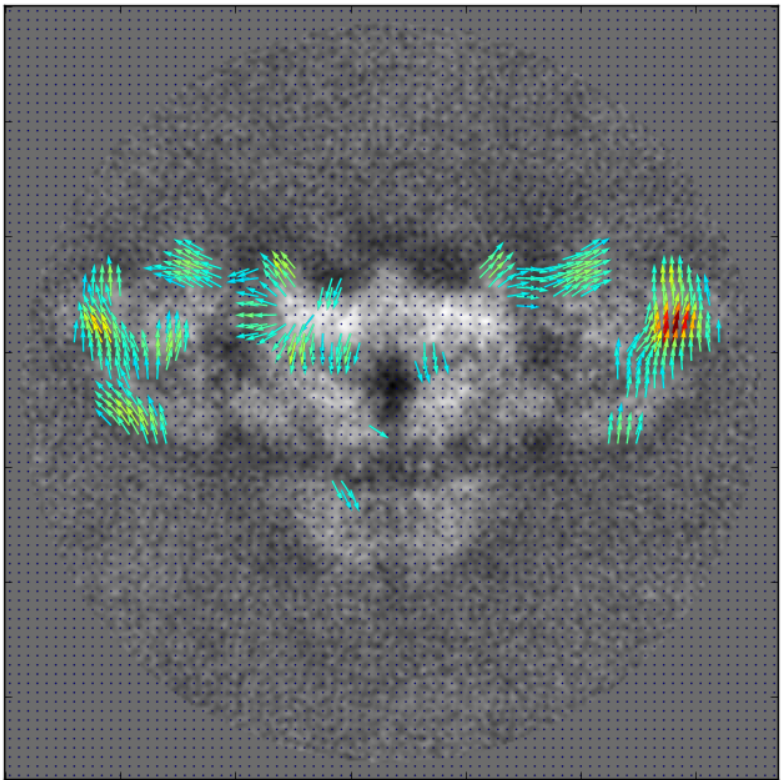

Figure 3: Example output file of flow vectors from a single PD when *Export Optical Flow* is enabled. Image motion is expressed by the direction of the vectors, while the magnitude of the motions are expressed by the relative color of each vector (with red denoting the maximum magnitude of motion in the NLSA movie). The circular background region surrounding RyR1 was removed from computation via use of a spherical *Mask Volume*.

7.2 Find Conformational Coordinates

Once you have filled in the appropriate values for the parameters at the top of the *Compilation* tab, click the *Find Conformational Coordinates* button to initiate *Optical Flow* and *Belief Propagation* across your entire data set. These two procedures aim to select the correct eigenvector/sense combination for the user-defined conformational motion across all PDs. To achieve this, *Optical Flow* is first used to define the most prominent visual motions in the 2D NLSA movies in terms of feature vectors (based on a histogram of oriented gradients), which are calculated for every eigenvector/sense combination across all PDs. Next, the set of all feature vectors in each PD is compared to the set of all feature vectors in its immediate neighbors on the S^2.

Belief Propagation assesses the affinity between all pairwise-combinations of feature vectors between all neighboring PDs, ultimately giving each comparison a likelihood score for how well it conserves the intended conformational motion (defined by the PD anchors). These probabilities are propagated across the network of PDs until uncertainty is minimized on the global scale. After this process has been completed, you can check these eigenvector/sense assignments within the output

file located at: `outputs_<project name>/CC/comp_psi_sense_nodes.txt`, and compare the fidelity of each PD's assignment with the motions you see in the respective movie on the *Eigenvectors* tab.

The ManifoldEM Python suite also includes a feature to automatically find erroneous PDs by analysis of τ statistics. In certain situations, we have found that certain 2D NLSA outputs do not converge depending on the images contained in a particular PD, and therefore generate 2D NLSA movies that are "bad" (i.e., very noisy, jittery or almost completely static). This is also reflected as a relatively discrete, narrow τ-value distribution for such movies. Our automation strategy uses the interquartile range (IQR) to characterize the dispersion of the τ histograms for all movies across all PDs. From the distribution of all IQR values, we automatically determine the cutoff IQR value which separates relatively well spread-out histograms from the narrow ones. When all of the movies for a given PD are below that IQR cutoff value, we automatically remove the PD from interfering with belief propagation and obstructing final outputs.

7.3 Energy Landscape

Within the *Energy Landscape* module, for each PD's chosen eigenvector, its corresponding τ parameterization is subdivided into 50 uniformly spaced bins (each representing a unique NLSA state), with the number of snapshots falling within each bin tallied towards its state's occupancy (as is visualized in the right-hand side figure under *Tau Analysis*).

In thermal equilibrium, we attribute differences in occupancy to differences in the molecules' free energy via the Boltzmann factor $\Delta G/k_B T = -\ln(n_s/n_0)$, where n_s is the number of snapshots in the current state and n_0 is the occupancy of the maximum-occupancy state in the state space (Fischer et al., 2010; Agirrezabala et al., 2012). The lowest observable occupancy in the ensemble represented by the dataset, of one particle in a state, defines the highest measured free energy while the highest observable occupancy defines the lowest measured free energy. The Boltzmann constant k_B is a physical constant that relates the average relative free energy of particles to their bulk temperature. (Please see the *Compilation Parameters* section for information on the temperature, T). The free energy of a state in this landscape is a thermodynamic quantity equivalent to the capacity of a system to do work. Finally, this occupancy/energy information is integrated across the chosen eigenvectors of all PDs, with the ordering of states within each defined via its *Sense*.

When only one degree of freedom is desired (or available), the NLSA occupancies and images corresponding to the same CC content in different PD manifolds can be further compiled across S^2 to construct a 1D energy path and a set of corresponding reconstructed volumes. Although not available in this Beta release, the NLSA procedure is more complicated when two degrees of freedom are desired. For completeness, we note that after identification of two CCs, their respective eigenvectors for the current PD manifold are used to isolate a 2D subspace therein. On this $\{CC_1, CC_2\}$ subspace, NLSA is performed independently along the directions of 180 uniformly-spaced radial lines in the range $\theta \in [0, \pi]$. This yields a collection of point densities (i.e., 1D occupancy maps) $n(\tau,\theta)$ for each θ. The collection of these 1D maps for all θ constitutes the 2D Radon transform

of a yet unknown 2D density map (i.e., the desired 2D occupancy map). An inverse Radon transform is then applied to reconstruct the 2D density map. In addition, NLSA also retrieves the noise-reduced images at each point in this map. As in the 1D case, this procedure must next be performed for the eigenvector pairs corresponding to $\{CC_1, CC_2\}$ in all other PD embeddings, from which noise-reduced volumes can be reconstructed to form 3D movies of concerted conformational motions.

7.4 Recompile Results

At any time after running *Find Conformational Coordinates* or *Energy Landscape* on the *Compilation* tab, you are given the option to recompile this information. This can be done via the *Recompile Results* button on the *Eigenvectors* tab (which was previously labelled *Compile Results* on the first run). Subsequent results will only change if you wish to change your previously assigned *PD Anchors*, *PD Removals*, *Dimensions* value (currently disabled in the Beta), or the *Temperature* value.

8 Energetics Tab

8.1 Energetics

The *Energetics* tab provides a visualization of the resulting energy landscape (i.e., 1D Energy Path, for the Beta release) as integrated across all PDs, with the dimensionality d defined via the number of chosen conformational coordinates (d=1 in this Beta release). Using the *View Distribution* button, you can switch views between the *1D Occupancy Map* and *1D Energy Path*, showing the difference between the initial occupancies across all PDs and the resulting transformation via the Boltzmann factor.

In the *1D Energy Path* representation, energetic wells represent the most energetically favorable conformations along your chosen conformational coordinate. Likewise, energetic peaks represent thermodynamically improbable states which constrain transitions between neighboring wells. Given this context, if your energetics look biologically unnatural (completely flat as one example), you may want to recheck your anchor assignments on the *Eigenvectors* tab, with the possibility of redoing these calculations via the previously discussed *Recompile Results* button.

Before computing your 3D trajectory files along this conformational coordinate, you can change how the states will be combined along the given trajectory via the *Path Width* option. The default value (1) will result in 50 output image stacks, where each stack combines information only from projections belonging to the state it corresponds to (one stack per state). As this value is increased, a sliding window is introduced along the trajectory such that additional information from neighboring states is included when building each of the 50 image stacks. For example, choosing 3 for the *Path Width* will tell each image stack $\{1, \ldots, 50\}$ to include its own images along with those from its immediate neighbors; i.e., three microstates in total for each macrostate.

While not available in the Beta release, we provide here a glimpse of the 2D functionality of the Python ManifoldEM GUI, which is a work in progress. As is planned, depending on the previous choice of dimensionality, plots on the *Energetics* tab will be either 1D or 2D. In the case of 2D, the user will be presented with a subsequent choice to define a path through the 2D energy landscape (Figure 4). Using this interface, points can be added onto this 2D plot to form a custom path, with corresponding integrated energy recorded. Alternatively, the user can elect to export this energy landscape for analysis with external pathfinding programs – such as *POLARIS* (Seitz and Frank, 2020) – to potentially define a minimum-energy path of presumed biological significance. These trajectories can then be imported into the ManifoldEM GUI for use in its final computations. After a suitable path has been defined (if applicable), ManifoldEM will combine the NLSA movies from all states and PDs along that path into corresponding image stacks and alignment files. Post-processing modules, which are located external to the GUI in the ManifoldEM main folder hierarchy, can then be run to use the projections in these image stacks to reconstruct NLSA volumes. The final result of this framework is a sequence of successive 3D reconstructions along the chosen path, forming a 3D movie. In the case of the 1D Energy Path, this sequence demonstrates the conformational changes along a single CC.

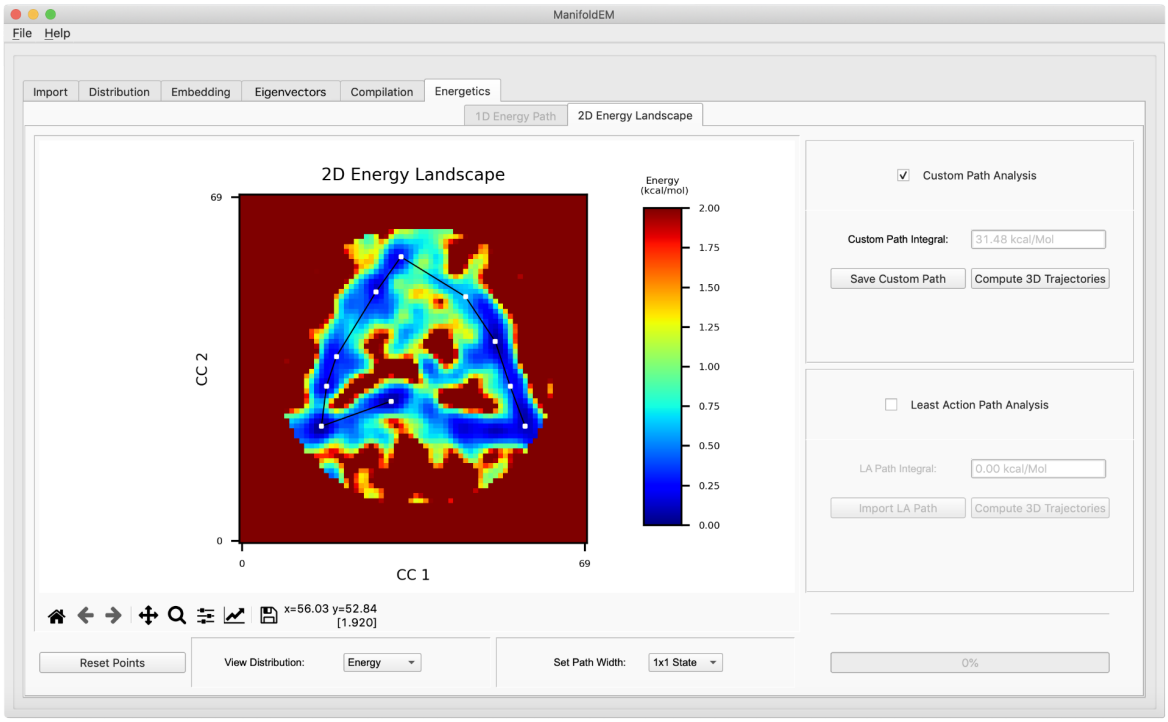

Figure 4: *2D Energy Landscape* tab showing outputs from the Ribosomal data set (Dashti et al., 2014), as viewed in Mac OS. A set of user-defined coordinates have been handpicked to form a path through the low-energy valley. This path can be used to generate the set of assets required to produce a final sequence of

NLSA volumes. Alternatively, the path of least action can be imported (as generated via external programs; e.g., *POLARIS*) and similarly used.

8.2 3D Trajectories

Once you have selected a suitable path width, press the *Compute 3D Trajectories* button. During this process, the images from all states across all PDs are combined into 50 image stacks and alignment files, such that there is one image stack and corresponding alignment file for each state along your trajectory. Each image stack {1, … , 50} contains all of the particles across S^2 that fall within its corresponding bin (state), with the angular information and microscopy parameters of each image written into that stack's alignment file.

9 Post-processing

After viewing the energy landscape (or energy path, for 1D) and computing 3D trajectories, a collection of image stacks (`.mrcs`) and corresponding alignment files (`.star`) will be exported into your `outputs_<project_name>/bin` directory. Each pairing in this collection coincides with one of the 50 conformational states for your chosen motion, with each state containing information from every PD across S^2.

9.1 Volume Reconstruction

With these files generated, an external algorithm (RELION) can next be used to reconstruct 50 volumes from this collection, representing a 3D movie displaying the chosen conformational motion. First, if you haven't yet installed RELION, do so now via the instructions in Appendix A. Once installed, navigate to the `outputs_<project_name>/post/1_vol` directory in the CLI, and run the batch-reconstruction script there via: `sh mrcs2mrc.sh`.

9.2 Noise Reduction

After your 50 volume files have been produced via RELION's reconstruction algorithm (as described in the previous section), you can elect to clean them via our external (to the GUI) post-processing scripts.

The first choice is via Singular Value Decomposition (SVD). The corresponding scripts are designed to decompose your volume sequence into a series of modes, and eliminate noise by removing modes below a singular value threshold. These two SVD scripts can be found in the `outputs_<project_name>/post/2_svd` directory and include `mrc2svd.sh` and `mrc2svd.py`. You can run both scripts at once by navigating to the above folder in the CLI (making sure the ManifoldEM Anaconda environment is also activated) and inputting the command: `sh mrc2svd.sh`. (To note, for volume files with large box sizes, these computations may take considerable time; e.g., hours). By default, the first and second eigenvector will be chosen as significant, and retained. During this initial run, a figure entitled `mrc2svd.png` will be saved, showing the eigenvalue spectrum for your data. After examining this plot, you can choose to rerun this procedure while retaining a different set of user-defined eigenvectors by first changing the `Topo_list` variable located at the top of `mrc2svd.py`, followed by again inputting the command `sh mrc2svd.sh`.

The second choice for noise reduction is via the `mrc2denoise.py` script, where either a Gaussian or median filter can be applied to each volume. As well, the window size of the filter and range of states on which the filter is applied can also be altered using the overhead parameters.

9.3 Rendering Animations

Below we provide two methods – either using Chimera or PyMOL – for rendering your 3D conformational changes in the form of movies from different 2D views.

For the Chimera workflow, we've provided two scripts to get you started in the `outputs_<project_name>/post/3_anim` directory: `1_CreateSession.py` and `2_GenMovie.py`

In the CLI, with both the ManifoldEM environment and Chimera sourced, run the first script via: `chimera 1_CreateSession.py` (change the `svd` variable inside to `True` if SVD was run in the previous step). This will load all 50 volumes into the Chimera user interface and subsequently hide them from view. You can next unhide one of your 50 volumes and choose a camera angle from which you'd like to view the 3D animation. After doing so, hide that volume again (such that all volumes are invisible in the *Volume Viewer*), and select *Save Session As* from the *File* menu. Uniquely name the session to correspond with this chosen view (e.g., `view1.py`), and save it within the `outputs_<project_name>/post/anim` directory.

Next, open the `2_GenMovie.py` file in editing mode, and change the `session` variable at the top of the script to correspond with your latest session name (e.g. `session = view1`). You can change many of the visualization options within this script if you're familiar with the Chimera syntax, but be careful to not introduce any logical conflicts. Once you're finished editing, run the script via `chimera 2_GenMovie.py`. This will tell Chimera to build an animated sequence from your chosen viewing angle, exporting it as both a `.png` sequence and `.mov` movie. This two-script workflow can be repeated for rendering animations from any number of viewing angles. If outputs appear noisy, try adjusting the settings for `step` and `hideDust` in `2_GenMovie.py`.

Users can also elect to follow our PyMOL workflow for viewing 3D movies of conformational change. For this procedure, first navigate to the `post/1_vol` directory in the CLI, where 50 volumes have been reconstructed. Next open PyMOL via the command `pymol` (or whichever CLI alias you have established). With the PyMOL GUI open, in the PyMOL command line, input the command:
`for idx in range(1,51):cmd.load("EulerAngles_1_%d_of_50.mrc"%idx,"mrc_mov")`

This will load all 50 volumes as a PyMOL sequence, which may take some time depending on the file sizes. Once loaded, you can change the mesh level of the volumes and other parameters to adapt to your visualization needs.

For users following along with the demo data set, we have provided a movie file in the `demo` directory – showing the RyR1 wing-like motion – for comparison with your final outputs.

10 Citing Us and Asking Questions

If ManifoldEM is useful in your work, please cite Dashti et al. (2014) and this ManifoldEM Python repository (available via Zenodo DOI, as shown in this repository's readme).

If you have any questions about ManifoldEM after reading this entire document, carefully check the ManifoldEM GitHub forum for similar inquiries or, if no similar posts exist, create a new thread detailing your inquiry. As well, if you find any errors while reading this document, please let us know. Our team is committed to support users in the months immediately following release. After which, the establishment of a continued support team cannot be guaranteed.

Appendix A: Notes on Installation

A.1 Install Anaconda environment

Below is a list of initial errors that may emerge while opening the GUI, along with potential solutions that have worked on a number of other workstations. We will continue to update this section as more issues are found (and solved).

- If a VTK error occurs while installing Mayavi, please review the Mayavi recommendations: https://docs.enthought.com/mayavi/mayavi/installation.html
- For Linux users, a specific library may need to be installed for MPI functionality. If errors occur during installation of `mpi4py`, before running `pip install mpi4py`, install the prerequisite library via: `sudo apt install libopenmpi-dev`. (Note that in our Beta release, MPI has not been fully tested).
- For Mac users, if a `no module named vtk` error arises during `pip install mayavi`, deactivate and remove the environment (via `conda deactivate` followed by `conda remove --name ManifoldEM --all`) and recreate via `conda create -n ManifoldEM python=3 vtk=9.0.1` (or for the latest vtk release)
- For Mac users, if an error arises during `pip install mpi4py`, try `conda install mpi4py`

If all else fails, check the GitHub forum and create a new thread if no relevant posts yet exist.

A.2 Install External Packages

RELION will need to be compiled if the binaries are not used. The pre-compiled version comes as a part of the CCPEM package suite (https://www.ccpem.ac.uk/download.php). For installing Chimera, binaries can be directly obtained on their web page. These packages require an initial registration and are free for research purposes.

Appendix B: Notes on GUI

B.1 CLI Arguments

The GUI can be initiated from the command line with optional arguments:

Resume project: use `--input str`; `str` is the project name (as located in the `<name>` string found in that project's `params_<name>.pkl`):

```
python manifoldEM_GUI.py --input str
```

Initiate MPI: use `--mpi str`; `str` is the full path to the machinefile:

```
python manifoldEM_GUI.py --mpi str
```

Your machinefile should be a text file containing the name of your nodes. The total number of nodes is specified as the number of processors input into the GUI on the *Embedding* tab. (Note that the use of MPI has not been fully tested in the Beta release).

B.2 Camera Controls

Below are a number of useful operations for navigating the 3D visualizations, as seen on the *Distribution* tab, *Eigenvectors* tab, and (for 2D) the *Energetics* tab.

B.2.1 Rotating

To rotate a 3D object, place the mouse pointer on top of the visualization window, and keep the mouse button pressed while dragging in the appropriate direction. An in-plane rotation can also be performed by rotating as above while holding down the control-key.

B.2.2 Zooming

To zoom in and out of the scene, place the mouse pointer inside the visualization window, and keep the right mouse button pressed while dragging the mouse upwards or downwards. If available, the mouse scroll wheel can also be used.

B.2.3 Panning

To translate the center of the scene, keep the left mouse button pressed in combination with holding down the shift-key while dragging the mouse in the appropriate direction. If available, the middle mouse button can also be pressed while dragging the mouse to pan in the appropriate direction.

B.2.4 Keyboard

If problems arise between scene navigation and cursor movement, a nonstandard key may have been pressed. Pressing the t-key (trackball mode) while hovering over the figure may reset this behavior. For more information on using Mayavi, including other keyboard shortcuts, please visit: http://docs.enthought.com/mayavi/mayavi/application.html

Appendix C: Preprocessing

If you're using your own experimental data set, it's possible that collections of erroneous information (such as misassigned particles or images of experimental artifacts) are stored within an isolated PD or among your other images in numerous PDs. In cases of these "garbage dumps", problems can emerge for erroneous PDs during the proceeding dimensionality reduction steps. If you find yourself running into errors on the *Embedding* tab, you may want to consider performing additional cleaning on your data set before running ManifoldEM.

Both 2D and 3D Classification (via RELION) may prove helpful, but in our tests with these algorithms, we've found that they can actually miss hundreds of erroneous images. In this event, an ad hoc hand-picking method may be more favorable. To begin, in RELION, navigate to *Subset Selection* and select your STAR alignment file under *I/O*. For other options, turn recentering, regrouping, subsets, and duplicates all off. Next, click *Run*, and in the subsequent subwindow, set: *Scale* = `1`; *Sigma contrast* = `0`; *Black value* = `0`; *White value* = `0`; *Display* = `rlnImageName`; *Sort images on* = `True`, `rlnLogLikelContribution`; *Reverse sort* = `True`; *Max number of images* = `-1`.

Depending on your number of snapshots, this may take a while to load. After loading, the images in this new window are ranked according to their likelihood contributions. Within this ranking, we've found that the worst-behaved snapshots reside at the tailends of this distribution; either at the very top of this ranked stack or at the very bottom. Therefore, we advise that users go through both tails and hand-select all particles that look erroneous.

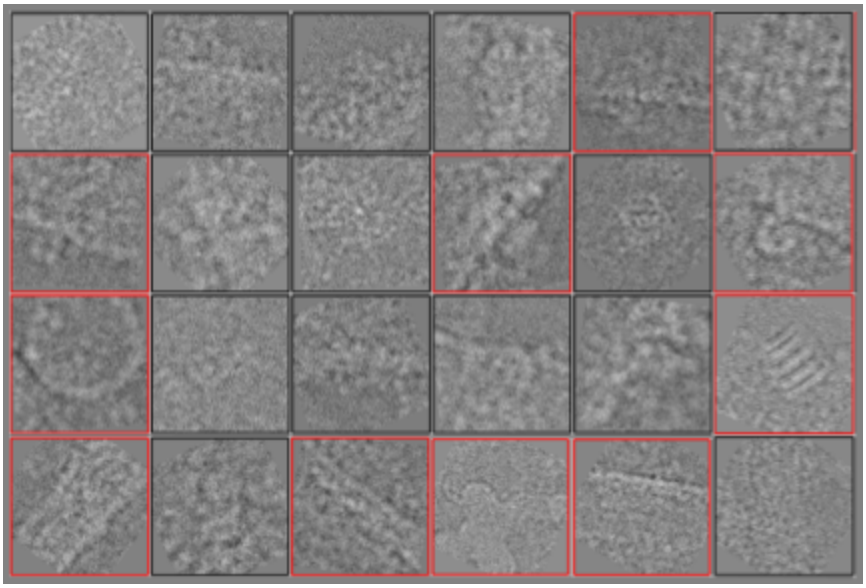

Figure 5: A few examples of problematic images are shown (demarcated with red boxes) from the V-ATPase cryo-EM data set obtained from Zhao et al. (2015), and include presence of ice sheets, amorphous blobs, and

densely-packed macromolecules. Such images were manually removed from the V-ATPase image stack before input into ManifoldEM.

Once you have selected the erroneous particles in both tail regions of this distribution, right-click anywhere within the window and select *Invert selection*. Next, right-click again and click *Save STAR with selected images*. You will then be prompted to save a new STAR file, after which, 3D Auto-Refine can be (optionaly) repeated with this newly cleaned data set to obtain a better calibrated alignment file for use in ManifoldEM.

Appendix D: External Data Viewers

A number of scripts for external visualization of data (outside of the ManifoldEM GUI) can be found in the `data_viewers` folder (located in the main directory). A brief guide to using these scripts is provided in each of their headers. The scripts `selecGCs_viewer.py`, `getDistances_viewer.py`, `DM_viewer.py`, and `psiAnalysis_viewer.py` can each be used to view data obtained after running the respective modules in the GUI (i.e., outputs from tessellation binning, distance calculations, diffusion maps, and spectral analysis, respectively). The `collageViewer.py` script can be used to create a 2x4 grid of animated NLSA movies (one for each PD) in the form of `.gif` files. This option may prove useful when assigning eigenvectors and senses (if working remotely) and for efficiently sharing dynamic information with collaborators.

Appendix E: Limitations and Uncertainties

We caution the user to potential issues found in the current ManifoldEM methodology, which have not been resolved as of this initial release.

E.1 Boundary Problems

The final 1D occupancy map and corresponding free-energy path obtained by combining individual PDs for a given CC displays a prominent, irregular pattern near the boundaries, regardless of data set. Specifically, there is a substantial, unaccounted increase in occupancies of states along each CC nearest the peripheral regions. The inconsistencies near each boundary of the 1D occupancy map first emerge in each PD individually, and thus also accumulate in the overall, combined occupancy map for all PDs and corresponding free-energy landscape. While in experimental data sets, we have found that roughly 5-10% (on average) of the states near the boundaries are affected, for synthetic data (Seitz et al., 2019), these occupancy misassignments were found to be nearly four times the expected value – covering a region of around 15% of states on both sides.

Importantly, these boundary characteristics result in biophysically-unrealistic deep free-energy wells at the border regions of the landscape. When generating 2D occupancy maps, with two such CCs in one map, these trends occur in the four corners of the plane. In the event that an energetic route encroaches into these regions, care must be given to these discrepancies. These boundary aberrations further manifest as confused conformational variation signals in the corresponding 3D NLSA maps, and for each, may prove inadequate for modeling a set of cohesive atomic-coordinate structures.

E.2 CC Ambiguity

The following prongs pertain to limitations and uncertainties encountered when comparing the NLSA outputs for each PD. Recall that NLSA produces an independent set of outputs for each PD-manifold eigenvector (for a delimited set of leading eigenvectors; e.g., eight). These outputs include (but are not limited to) a 2D NLSA movie and corresponding 1D occupancy map. By inspection of these 2D NLSA movies, decisions must be made to decide which eigenvectors represent a specific biologically-relevant CC, and assign to them a sense.

E.2.1 Duplicate CCs

In the set of NLSA outputs for each PD, the 2D NLSA movies along two different eigenvectors can sometimes be indistinguishable from one another (both visually and computationally), while providing significantly different occupancy distributions. Computational attempts to parse these CCs have included analysis via optical flow and an embedding of the furnished NLSA images

themselves into a new manifold for analysis of relevant features. The appearance of duplicate CCs with different energies is neither desirable nor biophysically feasible. As the ranking of each eigenvector (via the eigenvalue spectrum) represents the significance of each conformational variation signal in a given data set, the CC corresponding to the highest eigenvalue index should be typically chosen among duplicates. The case of identical types of CC content varying only in 2D motion amplitude has also been occasionally observed.

E.2.2 Aberrant CCs

Certain 2D movies may showcase hybrid and even physically-impossible motions, and must be rejected. For PDs where these occur, the biophysically correct CC choice is often (but not always) available. NLSA movies that show a "hybrid" motion appear to display a combination of two different motions, with each corresponding to two different CCs, as are observed from that same PD or neighboring PDs. As an example of a physically-impossible motion, Seitz et al. (2021) observed 2D movies (each corresponding to one eigenvector) obtained from synthetic data showing structural domains moving in different directions at the same time, which is physically impossible. User discretion (and subsequent validation) is therefore essential when considering the motions observed in each 2D NLSA movie.

E.2.3 Erroneous Movies

For certain eigenvectors corresponding to potential CCs within a given PD, the NLSA movies may appear to stall – broadcasting a series of identical frames over the course of its duration. The occurrence of NLSA movies with numerous pauses usually occurs due to confused NLSA manifolds (possibly due to insufficient image counts or the presence of aberrant or misaligned snapshots). For these eigenvectors, while the NLSA approach produces smoothly-varying and well-connected 1-manifolds, the resultant 2D movie is not smooth (i.e., featuring abrupt pauses).

E.3 CC Propagation

Errors in assignment of CCs and their senses may emerge during automation strategies present in the MEM Matlab and Python frameworks, with the latter (i.e., optical flow and belief propagation) observed to be significantly more accurate than the former (i.e., correlation coefficients). These errors can ultimately affect the quality of the final free-energy landscape and reconstructed 3D motions. As the CC propagation step (Maji et al., 2020) implements feature extraction methods which are applied to each of the NLSA movies to determine their similarity, its performance is thus naturally complicated by the presence of duplicate and aberrant CCs, as described above. In the absence of upstream errors, the optical flow routine has been found to capture motions with good accuracy, even under significant amounts of noise.

However, for data sets where the NLSA movies show relatively small, complex, or obscure motions (i.e., obscure as seen from a specific PD), the performance of optical flow computations can suffer, and as a consequence, its choice of CCs may be inaccurate (Maji et al., 2020). To remedy these

potential problems, the user-defined PD anchors must be chosen as judiciously as possible in order to obtain an accurate occupancy map and reconstructed 3D motion. As an added layer of supervision, the outputs of the Python automation strategy can be spot-checked after completion. If erroneous 3D motions are observed, the GUI allows previous decisions to be revisited, such that more PD anchors (or more accurate assignments) can be added to better guide these decisions.

E.4 Dampening of the 3D Motion Amplitudes

In several data sets, the reconstructed volumes representing a conformational change for each CC have been observed to show a dampened, reduced range of motion compared to the corresponding NLSA 2D movies from various PDs. The extent of this dampening has been found to vary with the data set. The extent of the 3D motion can appear dampened due to various factors, with this dampening not an issue to be solved in its own right, but actually the effect of some combination of upstream issues preceding it. The quality of the final 3D NLSA maps thus hinges on the accuracy of all preceding steps, within which the above-mentioned issues manifest and must be resolved. As a rough estimate, we have found the dampening to result in a third or less of the motion range as observed in the corresponding NLSA movies or via external studies. To note, for larger motions, we have also observed a smearing effect in the 3D structure of the domain under motion, which was most significant for our synthetic data (Seitz et al., 2019).

E.5 Manifold Outliers

In some PD manifolds outliers may appear which could affect the quality of conformational movies. Outlier points will appear significantly detached (a large distance away) from the typical body of each manifold, where the majority of points reside. These outliers could correspond to image artifacts or upstream misalignments. The GUI offers a tool – located within the eigenvector subwindow, per PD – to isolate and remove these potential outliers. After re-embedding, all NLSA movies (and corresponding manifold information) will be re-generated without the influence of these aberrant points.

E.6 Hyperparameter Tuning

Multiple parameters not controllable in the GUI may be needed in special circumstances. We detail a set of these most important hyperparameters, along with their file locations.

E.6.1 Manifold Tuning

For each embedding, there are a couple of parameters which can be set to obtain the optimum result: Number of nearest neighbors to be considered in distance calculation (`K`), Gaussian kernel width (`sigma` × `tune`). Currently, the `sigma` value is calculated using the method in Ferguson et al. (2010). The graphs associated with these calculations can be viewed for each PD in the GUI on the *Eigenvectors* tab, and may provide visual evidence of a suboptimal Gaussian bandwidth. K and tune have default values which we have found to be reliable, but there might be some cases where

adjusting them would give better results. Typically, the same parameters should be used for all PDs in a data set.

E.6.2 Concatenation Order

In NLSA, we can adjust the number of the images being concatenated. Increasing that number will reduce the amount of noise but also will reduce the range of conformational motions. The default value of `ConOrder` is set to work with typical Cryo-EM data sets. But in special cases, adjusting this parameter might be helpful.

E.6.3 Effective Dimensionality

The number of eigenvectors analyzed must be set large enough so as to capture the system's degrees of freedom. A constant value (e.g., the default `8` eigenvectors) will not always be sufficient for any given biological system. The only way to check the adequacy of this parameter is by viewing the generated 2D movies. In selected research, our default value has been sufficient for capturing the first two degrees of freedom in Ribosome (Dashti et al., 2014) and RyR1 (Dashti et al., 2020) data sets. While reliable for the Gaussian bandwidth estimations, we have recently found the method in Ferguson et al. (2010) – twice the slope of the sigmoid – to be an unreliable approximation for the effective dimensionality of PD datasets (Seitz et al., 2021). Calculation of the effective dimensionality is a longstanding issue in machine learning, and widely considered an open problem (Camastra and Staiano, 2016).

E.6.4 Aperture Index

The size of each tessellated bin can have a large impact on the ability to properly depict the conformational variation information in each PD. If these bins are too small, too few snapshots on average can be encapsulated within each PD. In contrast, if the bins are too large, orientational information may override conformational information discovered by NLSA. Our user manual contains a detailed guide to help better inform this decision, which is accessible via the GUI.

E.6.5 Lower Threshold

The minimum number of snapshots in each PD can be set in the GUI, and should be chosen with care. If too low, many PDs may be included with no useful conformational variation information. If set too high, too few PDs may be available to reliably reconstruct the final NLSA volumes.

All of the above issues have been observed in a range of data sets (experimental and synthetic, as generated via Seitz et al., 2019). Please see Seitz et al. (2021) for detailed descriptions of many of these issues and how they may arise. As well, we note again the forthcoming implementation of ESPER introduced by Seitz et al. (2021), which—given certain conditions in the quality of the data set are met—has been shown to circumvent many of these problems.

Appendix F: Bugs and Improvements

F.1 Known Bugs

- Mayavi display bug for 3D objects: https://docs.enthought.com/mayavi/mayavi/bugs.html
- Matplotlib `plt.Path` bug in `path.contains_points`: https://github.com/matplotlib/matplotlib/issues/9704
- Very large data sets can exceed the limits of `.pkl` files; suggest switching to `.h5` files instead
- The *Compare Movie* module can suffer from slowdowns if the NLSA movies from many PDs are viewed in sequence without exiting the subwindow. If such slowdowns occur, simply exit and reenter the window. The cause of this slowdown needs to investigated further
- If the *Spectral Analysis* progress bar stalls in the GUI for a significant amount of time (i.e., as understood by comparing with the creation dates and times of finished *Spectral Analysis* files in the `psi_analysis` folder), we first recommend simply restarting the GUI and resuming *Spectral Analysis* progress where it last left off. If you still find the same behavior as before, it is likely that one or more PDs has failed to converge. In this event, the `psiAnalysis_progress.py` script can be used to isolate these stalled PDs and print out the problematic eigenvector indices. This often occurs for PDs with confused information (possibly from erroneous upstream alignment assignments). To bypass these eigenvectors, close the GUI, and in the `psi_analysis/progress` folder, forcibly create progress files for each stalled $\{\mathrm{PD}_i,\Psi_i\}$ combination. It is imperative that you keep track of these new files, and, once the *Spectral Analysis* module is finished, mark the corresponding PDs as trash PDs on the next tab (via the corresponding GUI widget).

F.2 Future Improvements

Below is a list of potential improvements that could be made to the ManifoldEM suite, but have not been implemented as of this Beta release:

- Extend use to Windows OS (currently not tested).
- Complete testing of MPI.
- Incorporate GPUs.
- Add ability to run all initial steps—up to *Eigenvectors* tab—via CLI.
- Refactor code for easier maintenance.
- Update backend to read alignments in alternative (non-RELION) formats.
- Add option for elliptical defocus in backend.
- S^2 tessellated binning could be enhanced via adaptive bin sizes (based on the local densities of projections in angular space) or sliding window tessellations (thus creating a higher number of PD manifolds using overlapping information from previously-neighboring PDs).

- Explore use of image binning for faster computations (e.g., shrinking dimension of each image uniformly while retaining all core characteristics of the image).
- Automate discovery of optimal hyper parameters (see Section E.6).
- Standalone GUI for preprocessing images, specifically targeted to remove images that confuse distance calculations (e.g., images that are abnormally bright/dark or have harsh artifacts); see Appendix C.
- Add progress bar during *Resume Progress* and while reading `Data.py` on the *Imports* tab.
- Add file menu option (or alter use of original widget) for renaming projects.
- Add the ability to change the main volume or volume mask at any time.
- Add "gentle" data cleanup option in the file menu (e.g., as is done in RELION to remove extraneous files).
- The use of *Resolution* as a hyper-parameter may need to be readdressed. As is, the resolution of a 3D class average is not very informative for heterogeneous data sets.
- Add ability for users to add more eigenvectors (via *Embeddings* tab) at a later time. For example, if the user originally selects 5 eigenvectors and computes results, allow them the option to extend to 8, without having to recompute the first 5 from scratch.
- Add axis dropdown for the zeroth eigenvector for users to check for disconnected manifolds.
- `CC_Graph` needs to recompute the number of connected components before proceeding to the *Compilation* tab, since it is possible for the user to remove PDs in a fashion that creates newly isolated connected components. In this event, the user would then need to be given the option to add extra anchors in each newly formed island.
- Add ability to view angular distribution of all particles within a given PD.
- Provide a global method to remove trash PDs through choice of a custom *Low Threshold* on the *Eigenvectors* tab (similar to the use of *Low Threshold* for PDs on the *Distribution* tab).
- For 1D cases, a distinct folder for each conformational coordinate should be created (e.g., so as not to overwrite CC_1 if the user decides to backtrack and run 1D with CC_2).
- Add interface for multi-manifold mapping for data sets ±ligands, ±mutations or ±drugs.
- Standalone GUI for post-processing and analyzing final outputs of ManifoldEM. Include ability to display 3D animations of final volumes along different energy landscape trajectories, along with their local resolution (via heat map on each volume's surface). Additionally, create a 3D video player that allows users to rotate these animating volumes fluidly during playback. As well, create a user interface to clean up these volumes via filters and/or SVD (as is currently done via external code as described in Section 9).
- Energetics tab is currently only designed for 1 or 2 conformational coordinates; eventually expand both backend and frontend to handle 3 conformational coordinates (and higher).
- Incorporation of ESPER (see Seitz et al., 2021) to synthesize with outputs of current NLSA pipeline. For initial PD-manifold embeddings having pronounced geometric structure (as calculated by R^2 values above a given threshold in specific 2D subspaces), run ESPER instead of NLSA to retrieve high-quality images and a highly-accurate n-dimensional energy landscape. For all other PDs, use the NLSA pipeline to fill in structural information on S^2. Finally, reconstruct volumes using the outputs from these two disjoint sets of PDs, with each set exclusively calculated using NLSA or ESPER.

References

X. Agirrezabala, H. Liao, E. Schreiner, J. Fu, R. Ortiz-Meoz, K. Schulten, R. Green and J. Frank. Structural characterization of mRNA-tRNA translocation intermediates. *Proceedings of the National Academy of Sciences*, 109(16):6094—99, 2012.

F. Camastra and A. Staiano. Intrinsic dimension estimation: Advances and open problems. *Information Sciences*, 328(20):26—41, 2016.

R. Coifman and S. Lafon. Diffusion maps. *Applied and Computational Harmonic Analysis*, 21(1):5—30, 2006.

A. Dashti, P. Schwander, R. Langlois, R. Fung, W. Li, A. Hosseinizadeh, H. Liao, J. Pallesen, G. Sharma, V. Stupina, A. Simon, J. Dinman, J. Frank and A. Ourmazd. Trajectories of the ribosome as a brownian nanomachine. *Proceedings of the National Academy of Sciences*, 111(49):17492—97, 2014.

A. Dashti, G. Mashayekhi, M. Shekhar, D. Hail, S. Salah, P. Schwander, A. des Georges, A. Singharoy, J. Frank and A. Ourmazd. Retrieving functional pathways of biomolecules from single-particle snapshots. *Nature Communications*, 11(1):4734, 2020.

A. Ferguson, A. Panagiotopoulos, P. Debenedetti and I.G. Kevrekidis. Systematic determination of order parameters for chain dynamics using diffusion maps. Proc Natl Acad Sci USA, 107(31):13597—602, 2010.

N. Fischer, A. Konevega, W. Wintermeye, M. Rodnina and H. Stark. Ribosome dynamics and tRNA movement by time-resolved electron cryomicroscopy. *Nature*, 466(7304):329—33, 2010.

J. Frank, M. Radermacher, P. Penczek, J. Zhu, Y. Li, M. Ladjadj and A. Leith. SPIDER and WEB: processing and visualization of images in 3D electron microscopy and related fields. *Journal of Structural Biology*, 116(1):190—9, 1996.

J. Frank. *Three-Dimensional Electron Microscopy of Macromolecular Assemblies: Visualization of Biological Molecules In Their Native State*. Oxford University Press, Oxford, New York, 2006.

J. Frank. Generalized single-particle cryo-EM: a historical perspective. *Microscopy (Oxf)*, 65(1):3—8, 2016.

J. Frank. *Nobel Lecture: Single-Particle Reconstruction—Story in a Sample*. 2017.

A. Georges, O. Clarke, R. Zalk, Q. Yuan, K. Condon, R. Grassucci, W. Hendrickson, A. Marks, J. Frank. Structural basis for gating and activation of RyR1. *Cell*, 167(1):145—57, 2016.

D. Giannakis and A. Majda. Nonlinear Laplacian spectral analysis for time series with intermittency and low-frequency variability. *Proc Natl Acad Sci*, 109(7):2222—27, 2012.

M. van Heel, G. Harauz, E. Orlova, R. Schmidt and M. Schatz. A new generation of the IMAGIC image processing system. *Journal of Structural Biology*, 116(1):17—24, 1996.

L. Lovisolo and E. da Silva. Uniform distribution of points on a hyper-sphere with applications to vector bit-plane encoding. *IEEE Proceedings - Vision, Image and Signal Processing*, 148(3):187—93, 2001.

S. Maji, H. Liao, A. Dashti, G. Mashayekhi, A. Ourmazd and J. Frank. Propagation of conformational coordinates across angular space in mapping the continuum of states from cryo-EM data by manifold embedding. *J Chem Inf Model*, 60(5):2484—2491, 2020.

S. Maji and J. Frank. What's in the black box?—A perspective on software in cryo-electron microscopy. *Biophysical Journal*, 2021.

G. Mashayekhi. ManifoldEM Matlab repository. GitHub, 2020 (accessed Aug. 17, 2020). https://github.com/GMashayekhi/ManifoldEM_Matlab/

E. Seitz, F. Acosta-Reyes, P. Schwander and J. Frank. Simulation of cryo-EM ensembles from atomic models of molecules exhibiting continuous conformations. *bioRxiv*, 2019. doi: 10.1101/864116.

E. Seitz and J. Frank. POLARIS: Path of least action analysis on energy landscapes. *Journal of Chemical Information and Modeling*, 60(5):2581—90, 2020.

E. Seitz, F. Acosta-Reyes, S. Maji, P. Schwander and J. Frank. Geometric machine learning informed by ground truth: Recovery of conformational continuum from single-particle cryo-EM data of biomolecules. *bioRxiv*, 2021a. doi:10.1101/2021.06.18.449029.

T. Sztain, S. Ahn, A. Bogetti, L. Casalino, J. Goldsmith, E. Seitz, R. McCool, F. Kearns, F. Acosta-Reyes, S. Maji, G. Mashayekhi, J. McCammon, A. Ourmazd, J. Frank, J. McLellan, L. Chong and R. Amaro. A glycan gate controls opening of the SARS-CoV-2 spike protein. *Nature Chemistry*. 2021.

P. Whitford, R. Altman, P. Geggier, D. Terry, J. Munro, J. Onuchic, C. Spahn, K. Sanbonmatsu and S. Blanchard. *Dynamic Views of Ribosome Function: Energy Landscapes and Ensembles*. Springer, Vienna, 2011.

J. Zhao, S. Benlekbir and J. Rubinstein. Electron cryomicroscopy observation of rotational states in a eukaryotic V-ATPase. *Nature*, 532:241—5, 2015.

Contributions

Detailed contribution notes for the ManifoldEM Python suite have been supplied in the header of all scripts in our online repository. Direction and project administration were overseen by Peter Schwander, Abbas Ourmazd and Joachim Frank.

This user manual was written by E. Seitz. Review and editing was performed by E. Seitz, G. Mashayekhi, Hstau Liao, Suvrajit Maji, Peter Schwander*, Abbas Ourmazd* and Joachim Frank*.

Acknowledgements

We thank Ali Dashti, Sonya Hanson and Francisco Acosta-Reyes for support in several ManifoldEM endeavors related to this release. In addition, we appreciate the help and feedback of our alpha users, including Spencer Bliven, Andres de la Peña, Wen Ma, Salah Salah, Cecilia Casadei, Mrinal Shekhar and Andres Hernandez. This work was supported by NIH R01 GM 29169, R01 GM55440, and R35 GM139453 (to J.F.) and by the US Department of Energy, Office of Science, Basic Energy Sciences under award DE-SC0002164 (underlying dynamical techniques), and by the US National Science Foundation under awards STC-1231306 (underlying data analytical techniques) and DBI-2029533 (underlying analytical models) (to A.O. and P.S.).